J Mater Sci: Mater Electron **(2023) 34:1827**

In situ IV and CV characterization of Pt/n-GaN Schottky barrier diodes irradiated by 100 MeV oxygen ions

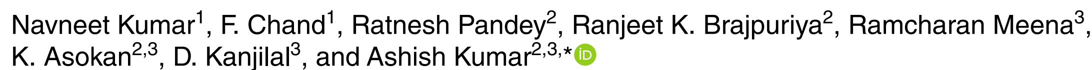
Navneet Kumar[1], F. Chand[1], Ratnesh Pandey[2], Ranjeet K. Brajpuriya[2], Ramcharan Meena[3], K. Asokan[2,3], D. Kanjilal[3], and Ashish Kumar[2,3,*]

[1] *Department of Physics, Kurukshetra University, Kurukshetra 136119, India*
[2] *Department of Physics (SoE), University of Petroleum and Energy Studies (UPES), Bidholi, Dehradun 248007, India*
[3] *Inter University Accelerator Centre, Aruna Asaf Ali Marg, Vasant Kunj, New Delhi 110067, India*

Received: 27 April 2023
Accepted: 28 August 2023
Published online:
20 September 2023

© The Author(s), under exclusive licence to Springer Science+Business Media, LLC, part of Springer Nature, 2023

ABSTRACT

Pt/n-GaN Schottky diodes were fabricated on metal organic chemical vapor deposition grown epitaxial GaN thin films. Temperature-dependent electrical characterizations current–voltage and capacitance–voltage were performed in the temperature range of 80–500 K. Barrier inhomogeneity calculations of the pristine Schottky barrier diodes were performed. Furthermore, these devices were irradiated with 100 MeV oxygen ions in fluencies ranging from 10^{10} to 10^{14} ions/cm^2. In situ current–voltage and capacitance–voltage measurements were performed after each fluence. The Schottky barrier height and ideality factor increased, whereas the carrier concentrations decreased with an increase in the ion fluence. The results were interpreted based on the thermionic emission model and energy loss mechanism of the ion beam in GaN.

1 Introduction

GaN-based Schottky barrier diodes (SBDs) have various technological applications in power electronics, optoelectronic devices, and space because of their unique properties such as wide bandgap, radiation hardness, high saturation velocity, and high breakdown voltage [1, 2]. It is essential to analyze the variation in the device parameters of the SBD, such as the ideality factor, Schottky barrier height (SBH), carrier concentration, and series resistance with temperature and ion irradiation for the sustainability of these devices working under variable temperatures and radiation harsh space applications. Metal–semiconductor (MS) contacts with large SBHs, high rectification efficiencies, and low reverse leakage currents are required in applications such as power rectifiers and HEMTs [3]. As specified by the Schottky–Mott model, the SBH depends on the metal work function and semiconductor electron affinity (4.1 eV for GaN) [3–5]. Platinum (Pt) metal is suitable for use as a Schottky contact on n-type GaN because of its high work function

Navneet Kumar and Ashish Kumar have contributed equally to this work.

Address correspondence to E-mail: ashish.kumar@ddn.upes.ac.in; dr.akmr@gmail.com

https://doi.org/10.1007/s10854-023-11227-7

(5.65 eV) and corrosion and oxidation resistance [3]. There is not much literature on in situ experimental investigations of swift heavy ion (SHI) irradiation, especially for the MS interface, which is the subject of the current work. Radiation affects the properties of GaN depending on the type of radiation energy and doping [6, 7]. According to previous reports, the production of point defects, their migration, and annihilation, as well as a few other parameters, influence the damage mechanism in GaN at keV energies [7, 8]. In the keV regime, ions are implanted in the near-surface region, whereas in the SHI regime (energy ≥ of 1 MeV/amu), ions reach the substrate in the epitaxial films [9]. As a result, controlled changes at the MS interface can be accomplished either by creating new defects or by annealing existing defects [8, 10]. Several reports have been published on temperature-dependent current transport in Silicon and GaAs-based Schottky diodes [11–13]. Variations in the ideality factor and SBH with the fluence in metal/n-GaN Schottky diodes have been reported [14–17]. These results are linked to the modification in the interface state density at the MS contact affected by heating and defect formation caused by irradiation. Recently, temperature-dependent current–voltage (*I*–*V*) and capacitance–voltage (*C*–*V*) characteristics of Ni/n-GaN SBDs were studied by Yildirim [18]. However, few reports on the effects of temperature and ion irradiation on Pt/GaN Schottky diodes, are available in the literature. One such report by Kumar et al. highlighted *I*–*V* characteristics and Hall effect measurements of a Pt/GaN Schottky diode at temperatures in the range of 200–380 K [16].

In this study, SBDs were fabricated using Pt metal and GaN epitaxial layer on a sapphire substrate. In situ *I*–*V* and *C*–*V* characterizations of Pt/n-GaN SBDs were performed to observe the variation in electronic parameters under the influence of varying temperatures in the range of 80–500 K and ion fluences of 100 MeV oxygen ion irradiation from 1×10^{10} to 1×10^{14} ions/cm^2.

2 Experimental

GaN epitaxial layer (~ 4 μm) used in the fabrication of the Schottky contacts were obtained by MOCVD technique μ grown on a c-plane sapphire substrate. Before fabrication, the GaN epitaxial layers were chemically cleaned sequentially using trichloroethylene, acetone, and isopropyl alcohol solutions in an ultrasonic bath for 10 min each followed by rinsing with deionized (DI) water for 5 min. Immediately before metallization, the oxide contaminant was removed by dipping the samples in a HCl:H_2O (1:1) solution for 1 min and then in DI water. Deposition of Pt films of 100 nm on the n-GaN epitaxial layer was carried out using an electron beam deposition system. The base pressure of deposition was 10^{-8} mbar. For the characterization, small indium ohmic contacts were planted on the diode samples at two opposite edges via soldering. The diodes were irradiated with 100 MeV oxygen ions using the Pelletron accelerator facility available at IUAC, New Delhi. The fluences of the ion beams varied from 1×10^{10} to 1×10^{14} ions/cm^2. The ion beam was focused at an angle of 7° to avoid channeling. In situ *I*–*V* and *C*–*V* characterization of the diodes were performed using an Agilent Semiconductor Analyzer. Before the irradiation experiments, temperature-dependent electrical characterizations were performed at various temperatures in the range of 80–500 K by increasing the temperature by 30 K in each step using an LN2 Optistat DNV cryostat and a temperature controller (Oxford Instruments ITC503).

3 Results and discussion

3.1 *I*–*V* characterization of Pt/GaN SBD

The *I*–*V* characteristics were determined by varying the temperature to analyze the variations in the SBD parameters. The reverse and forward bias characteristics of the Pt/n-GaN SBD at various temperatures ranging from 80 to 500 K are shown in Fig. 1a. A thermionic emission model was used to fit the experimental data [4, 5].

$$I = I_S\left[\exp\left(\frac{q(V - IR_S)}{\eta k_B T}\right) - 1\right], \quad (1)$$

where I_S, V, R_S, and η are the saturation current, bias voltage applied across the barrier, series resistance, and the ideality factor, respectively. The SBH expression is given by

$$\phi_B = \frac{k_B T}{q}\ln\left(\frac{AA^* T^2}{I_S}\right), \quad (2)$$

where T, A,ϕ_B, and A^* represent the temperature of the diode, effective area of the MS contact,

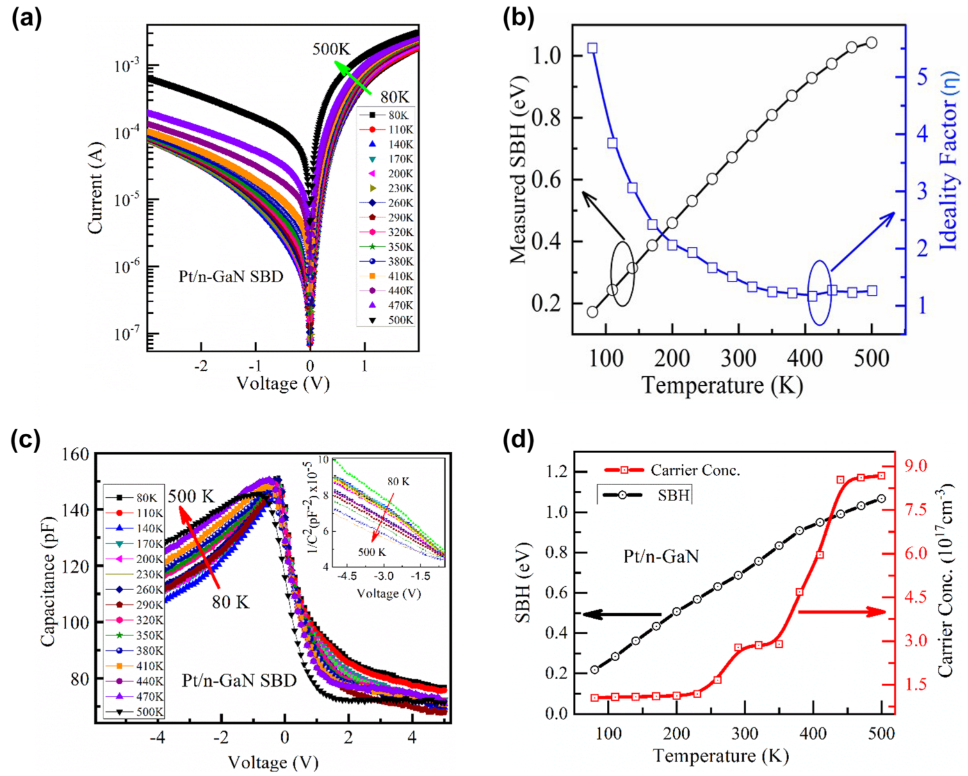

Fig. 1 **a** *I–V* characteristics of Pt/n-GaN SBD with varying temperature from 80 to 500 K, **b** variation of measured SBH and ideality factor with the temperature (based on *I–V*), **c** *C–V* curves of Pt/n-GaN SBD and inset shows $1/C^2$ vs. V curves for reverse bias voltage at a varying temperature in the range 80–500 K, and **d** variation of SBH and carrier concentration vs. temperature of Pt/n-GaN SBD (based on *C–V*)

barrier height, and the effective Richardson constant, respectively.

Using the above thermionic emission equation, the ideality factor η was calculated using the slope of the linear fit to the *I–V* characteristics between log(I) and V in the forward bias region. The intercept of the linear fit on the y-axis was expressed as the saturation current [19]. The SBH was calculated using Eq. (2). The series resistance was calculated from the forward *I–V* characteristics using the Cheung and Cheung method [20]. The diode parameters are listed in Table 1 and the changes in the SBH and η with temperature are shown in Fig. 1b. Ideality factor decreased from 5.5 to 1.24, while SBH increased from 0.17 to 0.81 eV, when temperature increased from 80 to 350 K. The increased value of η at lower temperatures indicates a deviation in the current transport from thermionic emission in the SBD [21]. This deviation might have occurred because of the presence of other current transport phenomena, such as tunneling and field emission [16]. At elevated temperatures, η improved and found to be 1.16 at 410 K. This means that the factor responsible for current transport, that is tunneling/field emission, decreased with increasing temperature. Another important parameter is SBH, which is related to the electric field developed at the MS junction. It also increased with increasing temperature. The calculated experimental data for the series resistance displayed in Table 1 show that it decreases with increasing temperature.

3.2 *C–V* characterization of Pt/GaN SBD

The *C–V* measurement of a SBD is dependent on temperature and is an important aspect of interest that can clarify the Fermi energy, built-in voltage, carrier concentration, and SBH. The variation in the capacitance of SBD can be expressed as follows [4, 5],

$$C = \sqrt{\frac{q\varepsilon_s\varepsilon_0A^2N_D}{2(V_{bi}+V)}} = \frac{\varepsilon_S}{w}, \tag{3}$$

where q is the electronic charge, ε_0 is the permittivity of free space, ε_s is the dielectric constant, A is the cross-sectional area of the contact, V_{bi} is the built-in voltage, and N_D is the carrier concentration. The capacitance of the diode was measured at 1 MHz. The *C–V* characteristic curves of the Pt/n-GaN SBD at various temperatures in the range of 80–500 K are shown in Fig. 1c. The carrier concentration was calculated using the slope obtained from the graph between $1/C^2$ and V according to the following equation as

Table 1 Calculated Schottky parameters with varying temperatures in the range of 80–500 K of Pt/n-GaN SBD from temperature dependent *I–V* and *C–V* analysis

	I–V analysis				*C–V* analysis	
Temp. (K)	SBH (eV)	Ideality factor	Rev. sat. cur. at – 1 V (μA)	$R_S(\Omega)$	SBH (eV)	Carrier conc. (N_d) ×10^{17} (cm^{-3})
80	0.17	5.50	7.77	647.9	0.22	1.05
110	0.24	3.84	7.67	647.2	0.28	1.07
140	0.31	3.06	8.12	601.2	0.36	1.08
170	0.38	2.41	8.27	600.7	0.43	1.10
200	0.46	2.05	8.69	577.8	0.50	1.12
230	0.53	1.93	9.10	566.7	0.56	1.18
260	0.60	1.66	9.73	551.6	0.63	1.65
290	0.67	1.50	10.8	540.4	0.68	2.77
320	0.74	1.32	11.8	533.1	0.75	2.85
350	0.81	1.24	13.2	530.6	0.83	2.89
380	0.87	1.22	14.9	530.0	0.90	4.68
410	0.93	1.16	19.0	534.4	0.94	5.95
440	0.97	1.26	31.7	533.9	0.99	8.53
470	1.02	1.23	52.5	528.6	1.03	8.60
500	1.04	1.26	166.0	520.7	1.06	8.67

$$N_D = \left(\frac{2V}{q\varepsilon_S A^2 * \text{slope}}\right) = \frac{2V}{q\varepsilon_S A^2 \frac{d(C^{-2})}{d(V)}} \quad (4)$$

and SBH related to built-in potential can be determined from the following equation

$$\phi_{ap} = \text{Intercept} * q\varepsilon_S A^2 \frac{N_d}{2} + \left(\frac{kT}{q}\right) \ln\left(\frac{N_c}{N_d}\right). \quad (5)$$

here Intercept is the intercept on the y-axis in the curve plotted between $1/C^2$ and V, and N_C is the effective charge state concentration in the conduction band. The parameters determined from the $C–V$ analysis are listed in Table 1 and shown in Fig. 1d. It can be seen from the data that there is an increment in carrier concentration from 1.05×10^{17} to 8.67×10^{17} cm^{-3} and in SBH from 0.22 eV to 1.06 eV as temperature increases from 80 to 500 K.

This type of dependence of the SBH on temperature is generally described in terms of the energy band gap of semiconductors, which can fluctuate with temperature. Nevertheless, in an actual Schottky diode, the temperature coefficient of the energy bandgap is often considerably different from that of the SBH. Many reports have specified various distinct causes for such non-ideal behaviors. Werner and Güttler reported that this type of behavior arises from Schottky barrier inhomogeneity [18, 22–24] present at the interface [25]. This inhomogeneity arises because of many factors, such as the diode fabrication process, material preparation, surface defect density, and local increase in the electric field, which can also cause a local reduction in the SBH. Consequently, the transport current became inhomogeneous. The ideality factor η greater than one in the $I–V$ curves results from the shape and location of the peaks in the potential barriers which are dependent on the bias voltage. Using the weighted data of the Gaussian distribution across all patches and the thermionic emission current expression with each value of SBH, the total current can be obtained in SBDs. The model indicates that the perceived SBH is consistently less than the barrier distribution' mean value and is given by the following equations [22, 26].

$$\phi_{ap} = \phi_{bo} - \frac{q\sigma_{SO}^2}{2kT}. \quad (6)$$

here ϕ_{ap} is the apparent SBH calculated in the forward region of the diode, and σ_{so} is the standard deviation of the SBH distribution at zero bias and the barrier homogeneity measure with negligible temperature dependence. ϕ_{bo} is the mean SBH at zero bias. By plotting the graph between ϕ_{ap} and $1/2kT$, we obtained the value ofσ_{so}^2 from the slope and ϕ_{bo} from the intercept. The variation in η is given as

$$(\eta^{-1} - 1) = -\rho_2 - \left({}^{q\rho_3}/_{2kT}\right). \quad (7)$$

The non-dependence of η on the bias requires a linear dependence of SBH and the square of the standard

deviation on the bias voltage. Parameters ρ_2 and ρ_3 are the voltage coefficients of the mean SBH and the standard deviation square, respectively. Details of the calculations can be found elsewhere [17]. Three sets of σ_{so}^2, ϕ_{bo}, ρ_2, and ρ_3 in the temperature ranges of 80–140 K, 170–260 K, and 290–500 K are shown in Fig. 2a. The linearity of the graph depicts adherence to the barrier inhomogeneity model.

Similarly, for the Richardson plot, the modified saturation current equation is given as

$$\ln\left(\frac{I_0}{T^2}\right) - \frac{q^2\sigma_{so}^2}{2k^2T^2} = \ln\left(AA^{**}\right) - \left(\frac{q\phi_{bo}}{kT}\right). \quad (8)$$

Using the above expression, a modified Richardson plot was obtained by plotting the LHS of the equation as a function of 1/kT. Using linear fitting, the modified Richardson constant was determined from the intercept and $\phi_{bo}$from the slope [27]. Theoretically, for n-GaN, A^{**} is 26.4 A/(cm^{2}K^2). Three plots were obtained for three values ofσ_{so}^2, and thus three different Richardson constants and SBH were obtained for three temperature ranges (80–140 K, 170–260 K, and 290–500 K), as listed in Table 2 and are shown in Fig. 2b [16]. When moving from the low-temperature range to the high-temperature range, the value of the Richardson constant also approached the theoretical value. These types of SBDs with large barrier heights are suitable for many power electronic applications.

3.3 Ion irradiation effect on Pt/GaN SBD

The samples were then irradiated at 300 K with 100 MeV oxygen ions using a Pelletron accelerator

Table 2 Calculated mean SBH, Richardson's constant from the barrier inhomogeneity model

Temperature range (K)	Mean SBH (eV)	Richardson's constant (A/cm^{2}K^2)
80–140	0.496	47.97
170–260	0.99	39.49
290–500	1.584	30.12

at IUAC, New Delhi. The *I–V* and *C–V* data were obtained at 300 K for ion fluencies ranging from 1×10^{10} to 1×10^{14} ions/cm^2. The analysis of the SBH and ideality factor was repeated using Eqs. (1–5), as explained above. An increase in the SBH and a decrease in η with increasing ion fluence were observed as shown in Fig. 3a. The parameters determined from the *I–V* analysis of the irradiated samples are listed in Table 3.

C–V data were obtained for the irradiated sample, and the carrier concentration was determined from the slope, whereas the SBH was obtained from the intercept of the $1/C^2$ vs. voltage (V) curves at different fluences. The changes in the carrier concentration and SBH with the fluence are shown in Fig. 3b. It was observed that SBH increased while the carrier concentration decreased with an increase in the ion fluence. The increase in the ideality factor and decrease in the carrier concentration with an increase in fluence can be easily understood because the ion beam is expected to cause damage at the MS interface as well as the bulk of GaN. However, most reported irradiation investigations with heavier

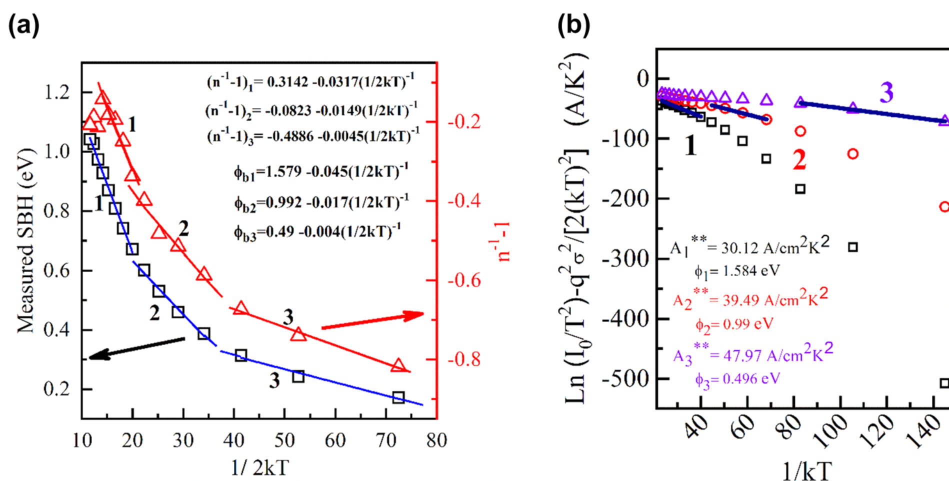

Fig. 2 **a** Variation of SBH (square symbol) and $\eta^{-1} - 1$ (triangle symbol) vs. 1/2kT curve (triangle symbol) of Pt/n-GaN SBD, **b** modified Richardson plot of $\left[\ln\left(\frac{I_0}{T^2}\right) - \frac{q^2\sigma_{so}^2}{2k^2T^2}\right] vs \frac{1}{kT}$. Three plots were obtained for three values σ_{so}^2 as represented by the symbols triangle, circle, and square for given temperature ranges (80–140 K, 170–260 K, and 290–500 K), respectively

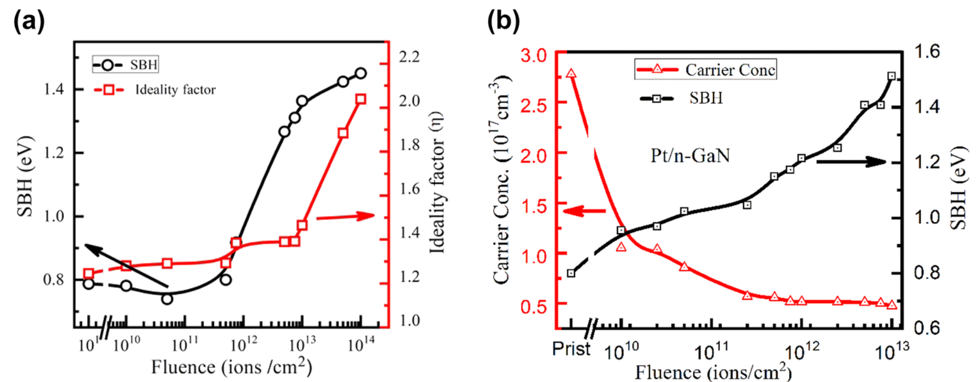

Fig. 3 **a** Variation in SBH and η (from IV) of irradiated Pt/n-GaN SBD with ion irradiation fluence, **b** SBH and carrier concentration versus fluences at temperature 300 K measured from *CV* measurement

Table 3 Calculated parameters of irradiated Pt/n-GaN SBD from *I–V* and *C–V* characteristics.

Fluence (ions/cm^2)	*I–V* analysis		Fluence (ions/cm^2)	*C–V* analysis	
	Ideality factor	SBH (eV)		Carrier conc. (cm^{-3})	SBH (eV)
Pristine	1.24	0.79	Pristine	2.77×10^{17}	0.80
1×10^{10}	1.28	0.78	1×10^{10}	1.05×10^{17}	0.95
5×10^{10}	1.29	0.74	2.5×10^{10}	1.04×10^{17}	0.97
5×10^{11}	1.29	0.80	5×10^{10}	8.58×10^{16}	1.02
7.5×10^{11}	1.38	0.92	2.5×10^{11}	5.71×10^{16}	1.05
5×10^{12}	1.39	1.27	5×10^{11}	5.59×10^{16}	1.15
7.5×10^{12}	1.40	1.31	7.5×10^{11}	5.20×10^{16}	1.17
1×10^{13}	1.46	1.36	1×10^{12}	5.17×10^{16}	1.22
5×10^{13}	1.88	1.42	2.5×10^{12}	5.16×10^{16}	1.25
1×10^{14}	2.04	1.45	5×10^{12}	5.13×10^{16}	1.41
			7.5×10^{12}	5.02×10^{16}	1.41
			1×10^{13}	4.77×10^{16}	1.51

The blank spaces in this table indicate the unavailability of results due to the presence of noise in the system

ions (200 MeV Ag and 150 MeV Au) in GaN devices showed a decrease in the SBH values after irradiation [28–31]. The present SBH trend can only be understood by considering the oxygen ion-GaN interaction mechanism in detail. When an ion enters a material, it loses energy via two mechanisms electronic energy loss (S_E) and nuclear energy loss (S_N). For oxygen ions (100 MeV), the former loss mechanism is dominant in epitaxial GaN thin films (< 5 µm thick). The nuclear energy loss process dominates only at the end of the ion range, which is in the sapphire region in the present samples. Because of this energy transfer, the GaN lattice temperature spikes for a very short duration. However, the maximum lattice temperature reached for the 100 MeV oxygen ion is ~ 530 K, which is significantly lower than the melting point of GaN (2773 K) [32]. Thus, no local melting or permanent cluster/track formation occurred for oxygen ions in the present case. Furthermore, a simple SRIM/TRIM calculation for 100 MeV oxygen ions in GaN showed that each oxygen ion created approx. 9.5 vacancies. This shows that small point defects were still produced, which might contribute to the electrically active defect states (charge trap levels and scattering centers) in the bandgap. As a result, the carrier concentration and conductivity of GaN decreased with increasing fluence, as observed in our case. The measured value of SBH (φ_{ap}) is given as the difference between the ideal barrier height (φ_b) *and* Schottky barrier lowering factor ($\Delta\varphi_b$), that is, $\varphi_{ap} = \varphi_b - \Delta\varphi_b$. Factor $\Delta\varphi_b$ depends on the carrier (dopant) concentration of the sample ($\propto (N_D^+)^{1/4}$) [5, 28, 29]. The decrease in N_D^+ with irradiation fluences results in a reduced $\Delta\varphi_b$ factor, and hence, an increased value of SBH at higher fluence values. At higher fluences, the accumulated defects degrade

device properties by providing leakage paths, and alternate transport mechanisms. The increased value of the ideality factor is a clear indication of the presence of a non-thermionic emission current transport mechanism. For GaN-based SBDs irradiated by heavier ions (Ag and Au), defect accumulation and device degradation begin at much lower fluences because the energy transferred to the lattice per ion is much larger [30–33].

4 Conclusion

Pt/n-GaN Schottky diodes were fabricated and investigated using temperature-dependent *I*–*V* and *C*–*V* measurements. An increase in the SBH and a reduction in the ideality factor were observed, whereas the series resistance decreased with increasing temperature. Barrier inhomogeneity was observed in the samples, as the diode samples exhibited different mean barrier heights under different temperature regimes. The Richardson's constant was found to be close to the theoretical value of 26.4 $A/cm^2 K^2$ in the temperature range of 290–500 K. In situ irradiation studies of the device with oxygen ions (100 MeV) showed that the SBH enhanced in both the *C*–*V* and *I*–*V* analysis as the fluence of irradiation increased. The ideality factor and carrier concentration determined from the *C*–*V* analysis decreased with increasing fluence. A better understanding of the defect evolution in GaN-based devices in harsh environments with high temperatures and radiation is necessary for potential low-earth satellite applications. Further studies with different ion types and energies are required to fully understand the mechanism and predict device behavior and lifetime for such applications.

Acknowledgements

AK would like to acknowledge the financial help from DST India in the form of a DST INSPIRE faculty grant. AK would also like to thank IUAC New Delhi for providing the beam time support.

Author contributions

NK: performed the electrical measurements, analyzed the results, and wrote the manuscript. AK: planned the investigation, performed the in situ measurements, and helped in writing the manuscript. RP: and RB: helped with analysis and manuscript review. RM and KA: provided assistance in situ measurements. FC and DK: provided mentorship and revised the manuscript.

Data availability

Data supporting the findings of this manuscript are available from the corresponding author upon reasonable request.

Declarations

Conflict of interest I, corresponding author, declare that we have no known competing financial interests or personal relationships that could have appeared to influence the work reported in this paper.

Ethical approval The study was approved by the Ethics Committee of Inter University Accelrator Centre (IUAC), New Delhi, India. There was not done any experiment involving humans and animals.

References

1. J. Ajayan et al., A critical review of AlGaN/GaN-heterostructure based Schottky diode/HEMT hydrogen (H2) sensors for aerospace and industrial applications. Measurement. **186**, 110100 (2021)
2. M. Reddeppa et al., Current–voltage characteristics and deep-level study of GaN nanorod Schottky-diode-based photodetector. Semicond. Sci. Technol. **36**(3), 035010 (2021)
3. H. Morkoç, *Handbook of nitride semiconductors and devices* (Wiley, Hoboken, 2008)
4. E.H. Rhoderick, R.H. Williams, *Metal–semiconductor contacts* (Oxford University Press, Oxford, 1988)
5. S.M. Sze, K.K. Ng, *Physics of semiconductor devices* (wiley, Hoboken, 2006)
6. S.O. Kucheyev, J.S. Williams, S.J. Pearton, Ion implantation into GaN. Mater. Sci. Eng. R-Rep. **33**(2–3), 51–107 (2001)
7. S.O. Kucheyev et al., Deformation behavior of ion-beam-modified GaN. Appl. Phys. Lett. **78**(2), 156–158 (2001)

8. S.O. Kucheyev et al., Damage buildup in GaN under ion bombardment. Phys. Rev. B **62**(11), 7510–7522 (2000)
9. S.O. Kucheyev et al., Lattice damage produced in GaN by swift heavy ions. J. Appl. Phys. **95**(10), 5360–5365 (2004)
10. P.A. Karaseov et al., Density of displacement cascades for cluster ions: an algorithm of calculation and the influence on damage formation in ZnO and GaN. Semiconductors. **43**(6), 691–700 (2009)
11. S. Parui et al., Temperature dependent transport characteristics of graphene/n-Si diodes. J. Appl. Phys. **116**(24), 244505 (2014)
12. S. Verma et al., Situ investigation of current transport across Pt/n-Si (100) Schottky junction during 100 MeV ni^{+7} ion irradiation. IEEE Trans. Device Mater. Reliab. **13**(1), 98–102 (2012)
13. M. Hudait, P. Venkateswarlu, S. Krupanidhi, Electrical transport characteristics of Au/n-GaAs Schottky diodes on n-Ge at low temperatures. Solid State Electron. **45**(1), 133–141 (2001)
14. V. Baranwal et al., Effect of ion irradiation on current–voltage characteristics of Au/n-GaN Schottky diodes. J. Alloys Compd. **480**(2), 962–965 (2009)
15. A. Kumar et al., Electrical and microstructural analyses of 200 MeV Ag^{14+} ion irradiated Ni/GaN Schottky barrier diode. Appl. Phys. Lett. **101**(15), 153508 (2012)
16. A. Kumar et al., Temperature dependence of electrical characteristics of Pt/GaN Schottky diode fabricated by UHV e-beam evaporation. Nanoscale Res. Lett. **8**(1), 1–7 (2013)
17. A. Kumar, S. Vinayak, R. Singh, Micro-structural and temperature dependent electrical characterization of Ni/GaN Schottky barrier diodes. Curr. Appl. Phys. **13**(6), 1137–1142 (2013)
18. N. Yıldırım, K. Ejderha, A. Turut, On temperature-dependent experimental *I–V* and *C–V* data of Ni/n-GaN Schottky contacts. J. Appl. Phys. **108**(11), 114506 (2010)
19. Ä. Dökme, The analysis of *I–V* characteristics of Schottky diodes by thermionic emission with a gaussian distribution of barrier height. Microelectron. Reliab. **51**(2), 360–364 (2011)
20. S. Cheung, N. Cheung, Extraction of Schottky diode parameters from forward current–voltage characteristics. Appl. Phys. Lett. **49**(2), 85–87 (1986)
21. S. Chand, An accurate approach for analysing an inhomogeneous Schottky diode with a gaussian distribution of barrier heights. Semicond. Sci. Technol. **17**(7), L36 (2002)
22. J.H. Werner, H.H. Güttler, Barrier inhomogeneities at Schottky contacts. J. Appl. Phys. **69**(3), 1522–1533 (1991)
23. E. Kalinina et al., Schottky barriers on n-GaN grown on SiC. J. Electron. Mater. **25**(5), 831–834 (1996)
24. Y. Song et al., On the difference in apparent barrier height as obtained from capacitance–voltage and current–voltage–temperature measurements on Al/p-InP Schottky barriers. Solid State Electron. **29**(6), 633–638 (1986)
25. Ã. Güllü et al., Electrical characterization of the Al/new fuchsin/n-Si organic-modified device. Phys. E: Low-Dimens. Syst. Nanostruct. **42**(5), 1411–1416 (2010)
26. R.T. Tung, Recent advances in Schottky barrier concepts. Mater. Sci. Eng. R-Rep. **35**(1–3), 1–138 (2001)
27. C. Crowell, The Richardson constant for thermionic emission in Schottky barrier diodes. Solid State Electron. **8**(4), 395–399 (1965)
28. S. Kumar et al., Influence of swift heavy ion irradiation on electrical characteristics of Au/n-Si (1 0 0) Schottky barrier structure. J. Phys. D **40**(22), 6892 (2007)
29. R. Singh, S. Arora, D. Kanjilal, Swift heavy ion irradiation induced modification of electrical characteristics of Au/n-Si Schottky barrier diode. Mater. Sci. Semiconduct. Process. **4**(5), 425–432 (2001)
30. A. Kumar et al., Dynamics of modification of Ni/n-GaN Schottky barrier diodes irradiated at low temperature by 200 MeV Ag^{14+} ions. Appl. Phys. Lett. **104**(3), 033507 (2014)
31. A. Kumar et al., Identification of swift heavy ion induced defects in Pt/n-GaN Schottky diodes by in situ deep level transient spectroscopy. Semicond. Sci. Technol. **33**(8), 085008 (2018)
32. A. Kumar et al., In situ transport and microstructural evolution in GaN Schottky diodes and epilayers exposed to swift heavy ion irradiation. J. Appl. Phys. **123**(16), 161539 (2018)
33. A. Kumar et al., Defect formation in GaN epitaxial layers due to swift heavy ion irradiation. Radiat. Eff. Defects Solids. **166**(8–9), 739–742 (2011)

Publisher's Note Springer Nature remains neutral with regard to jurisdictional claims in published maps and institutional affiliations.

Springer Nature or its licensor (e.g. a society or other partner) holds exclusive rights to this article under a publishing agreement with the author(s) or other rightsholder(s); author self-archiving of the accepted manuscript version of this article is solely governed by the terms of such publishing agreement and applicable law.